Investigation of the guided-mode characteristics of hollow-core photonic band-gap fibre with interstitial holes*

Yuan Jin-Hui(苑金辉)[a)†], Yu Chong-Xiu(余重秀)[a)], Sang Xin-Zhu(桑新柱)[a)],
Zhang Jin-Long(张锦龙)[a)], Zhou Gui-Yao(周桂耀)[b)],
Li Shu-Guang(李曙光)[b)], and Hou Lan-Tian(侯蓝田)[b)]

[a)] *Key Laboratory of Information Photonics and Optical Communications of Ministry of Education, Beijing University of Posts and Telecommunications, P.O. Box* 163, *Beijing* 100876, *China*

[b)] *Institute of Infrared Optical Fibres and Sensors, College of Information Science and Engineering, Yanshan University, Qinhuangdao* 066004, *China*

(Received 20 June 2010; revised manuscript received 5 January 2011)

This paper investigates the guided-mode characteristics of hollow-core photonic band-gap fibre (HC-PBGF) with interstitial holes fabricated by an improved twice stack-and-draw technique at visible wavelengths. Based on the simulation model with interstitial holes, the influence of glass interstitial apexes on photonic band-gaps is discussed. The existing forms of guided-mode in part band gaps are shown by using the full-vector plane-wave method. In the experiment, the observed transmission spectrum corresponds to the part band gaps obtained by simulation. The fundamental and second-order guided-modes with mixture of yellow and green light are observed through choosing appropriate fibre length and adjusting coupling device. The loss mechanism of guided-modes in HC-PBGF is also discussed.

Keywords: hollow-core photonic band-gap fibre, interstitial holes, guided-mode characteristics, full-vector plane-wave method

PACS: 42.81.–i, 42.81.Cn, 71.15.Ap **DOI:** 10.1088/1674-1056/20/6/064203

1. Introduction

Hollow-core photonic crystal fibres (HC-PCFs)[1,2] have attracted lots of attention over the past decade due to unique characteristics such as low propagation loss and high nonlinear threshold and so on. The exceptional characteristics have promoted many recent advances in gas-laser interactions such as ultra-low threshold stimulated Raman scattering in H_2-filled HC-PCFs[3] and electromagnetically induced transparency in molecular gases[4] and nonlinear optics of ultrashort pulses.[5,6] These fibres guide light of μm scale wavelength over kilometer scale distance through the light trapping in an air defect core relying on out-of-plane photonic band gap created by two-dimensional photonic crystal cladding structure or a low density of photonic states in Kagome-lattice structure.[7,8] The mode spectrum of hollow-core photonic band gap fibres (HC-PBGFs) arise from the waveguide properties of identified structural cladding constituents where the intersection between the guided-modes and cladding modes takes place, while the guided-modes in Kagome-lattice photonic crystal fibres (KLPCFs) occupy the same effective index space as the cladding modes without appreciably interacting with them.

Compared to KLPCFs, the characteristics of guidance and guided-modes in HC-PBGFs have been intensively investigated in theory and experiment. Cregan *et al.* first reported the air core guidance in higher-order band gaps lying in visible wavelengths in HC-PBGFs.[9] Bouwmans *et al.* analysed the mode properties of HC-PBGF at 850 nm, where the existing forms of different order guided-modes in the fundamental band gap were experimentally shown.[10]

*Project supported by the National Key Basic Research Special Foundation (Grant No. 2010CB327605), National High-Technology Research and Development Program of China (Grant No. 2009AA01Z220), the Key Grant of the Chinese Ministry of Education (Grant No.109015), the Discipline Co-construction Project of Beijing Municipal Commission of Education (Grant No. YB20081001301), and the Specialized Research Fund for the Doctoral Program of Beijing University of Posts and Telecommunications (Grant No. CX201023).

†Corresponding author. E-mail: yuanjinhui81@163.com

© 2011 Chinese Physical Society and IOP Publishing Ltd

Konorov *et al.* reported the dynamic propagation process of visible light in HC-PBGFs and showed the transverse field distributions.[11] Couny *et al.* deeply investigated the forming mechanism of band gaps and achieved the experimental visualization of the Bloch-modes in HC-PBGFs, where the relation between the guided-modes and cladding modes was indicated.[12] However, in the above reports, there were no interstitial holes existing in the cladding regions of HC-PBGFs and the influences of them on band-gap and guided-mode characteristics had not been involved. The guided-mode characteristics of HC-PBGFs with interstitial holes from near-infrared to visible wavelengths were analysed by us,[13−17] but more details of modes could not be distinguished because of longer fibre length and higher propagation loss. In this paper, guide-mode characteristics of HC-PBGF with interstitial holes at visible wavelengths are investigated. The transverse field distributions of different order guided-modes are theoretically shown and the corresponding propagation fields of fundamental and second-order guided-modes with yellow-green light are experimentally observed. The loss mechanism of guided-modes in band-gaps is elementarily discussed.

2. Simulation and experiment

The cross section of HC-PBGF designed and fabricated by the improved twice stack-and-draw technique[18,19] is shown in Fig. 1. As shown in Fig. 1(a), the whole cross section of HC-PBGF includes the outer cladding structure with diameter $D_1 = 305$ μm, which can couple the light energy into inner cladding region and decrease the leaky loss and the inner cladding structure with diameter $D_2 = 75$ μm, which can confine light energy in the air core. Figure 1(b) shows the amplified inner cladding structure and the corresponding structure parameters are as follows: the average cladding air hole diameter $d = 3.91$ μm, pitch $\Lambda = 4.03$ μm and core diameter $D = 15.2$ μm. Because of fluctuations of temperature and surface tension in the process of fabrication, the irregular cladding and interstitial holes are formed.

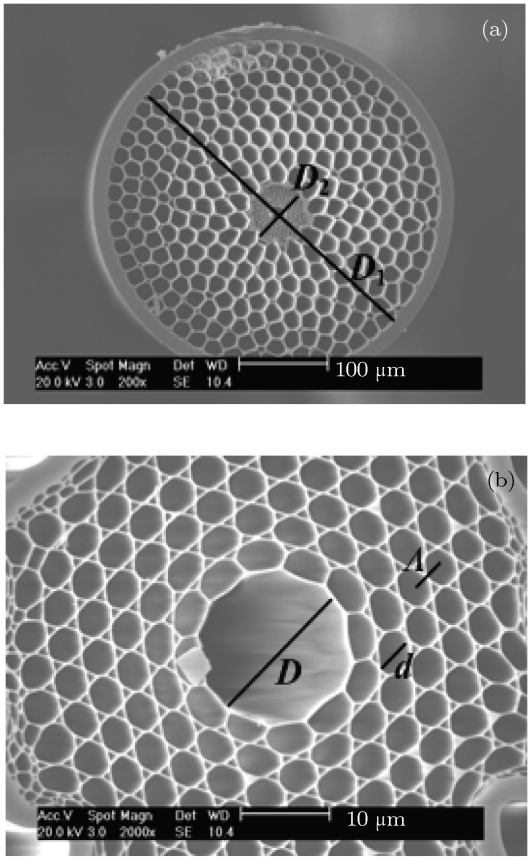


Fig. 1. (a) The whole cross section of HC-PBGF and (b) the amplified inner cladding structure.

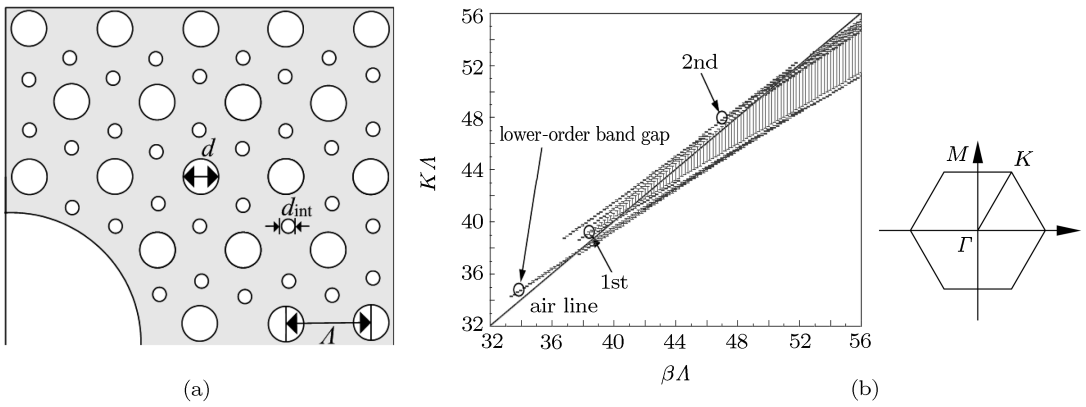


Fig. 2. (a) The cross-section structure of the model and (b) the normalized frequency $K\Lambda$ as a function of the normalized propagation constant $\beta\Lambda$. The 1st and 2nd photonic band gaps (PBGs) associated with the circles correspond to the different order band gaps considered, the lower-order band gap labeled by circle is unconsidered and the solid line represents the air line. Insert displays the first Brillouin zone symmetry point nomenclature.

All cladding and interstitial holes are considered to be regular circularity with the same sizes in order to simulate conveniently. Because of symmetrical structure, a quarter of the model cross-section is shown in Fig. 2(a). The chosen structure parameters are the cladding air hole diameter $d = 3.91$ μm, the interstitial holes diameter $d_{\rm int} = 0.65$ μm, the pitch $\Lambda = 4.03$ μm and the core diameter $D = 15.2$ μm. Based on the above model, the relation between normalized frequency $K\Lambda$ and normalized propagation constant $\beta\Lambda$ is presented in Fig. 2(b) by using the full-vector plane-wave method (FVPWM).[20,21]

As presented in Ref. [13], the resonance effect of glass interstitial apexes plays an important role in the forming of band gaps. With higher air filling fraction (above 95%), the interstitial apexes can be considered to be a series of isolated points distributing periodically in air and the light energy with the same wavelength scale will be scattered back into the air core. The characteristics of band gaps and guided-modes are primarily dependent on the interstitial apex sizes and the position of band-gaps will gradually shift to shorter wavelengths due to the existence of interstitial holes (the relation between the positions of band gaps and air filling fraction is shown in Ref. [13]). In Fig. 2(b), $K\Lambda$ is an approximately linear function with $\beta\Lambda$ varying from 32 to 56, the lower-order band gap is beyond consideration and the 1st and 2nd PBGs labeled are primarily considered. As presented in Fig. 2(b), the parts lying above air line of two PBGs with $K\Lambda > \beta\Lambda$ (the valid band gaps) exist in the $K\Lambda$ ranges of 38.6 to 49.5 and 47 to 52.3 and the corresponding wavelength ranges are from 511 nm to 656 nm and 484 nm to 536 nm. The photonic energy located in these valid PBGs can be propagated along the longitudinal direction in defect core due to existence of true photonic states. Furthermore, the propagation at a low loss in these valid PBGs, which arises from waveguide properties of identified structural cladding constituents, shows similar mode spectrum of the fibre cladding. However, while $K\Lambda < \beta\Lambda$ is satisfied (below air line), the photonic energy in PBGs will be distributed over the whole cladding region including air holes and glass structures, existing in the form of Bloch-modes because of weak guiding approximation. As shown in Ref. [11], different points of the reciprocal lattice in the first Brillouin zone have different contributions to the upper and down-edge forming of band gap. Because of two glass apexes existing within a primitive unit cell of the cladding crystal, the cladding modes at the Γ-point (as shown in insert of Fig. 2(b)) include symmetric or anti-symmetric modes. The symmetric modes (known as the modified fundamental space filling modes) form the upper-edge of the in-of-plane band gaps (below the air line) and are characterized by the fields in all the apexes being in-of-phase with one another. For anti-symmetric modes, they form the upper-edge of out-of-plane band gaps (above the air line). Instead of the whole PBGs, the guided-mode characteristics in part of 1st PBG, corresponding to the wavelength range of 575 nm to 589 nm ($\beta\Lambda$ changes from 43 to 44), is shown in Fig. 3.

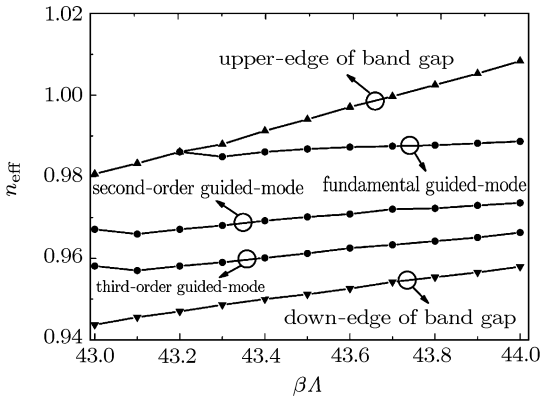


Fig. 3. The existing forms of different order guided-modes with $\beta\Lambda$ changing from 43 to 44. The dot line stands for the fundamental (HE_{11}), second-order (TE_{01} (TM_{01})) and third-order (HE_{31}) guided-mode and the up- and down-triangle line stands for upper- and down-edge of band gap.

According to the difference of effective refractive index $n_{\rm eff} = \beta\Lambda/K\Lambda$, the air guided-modes can be classified into the fundamental (HE_{11}), second-order (TE_{01} (TM_{01})) and third-order (HE_{31}) guided-mode. As illustrated in Fig. 3, when $\beta\Lambda$ changes from 43.2 to 44, the HE_{11} mode with $n_{\rm eff}$ above 0.985 can be well confined in air core and propagate along the longitudinal direction. When $\beta\Lambda$ changes from 43 to 44, the TE_{01} (TM_{01}) mode with $n_{\rm eff}$ below 0.975 has higher leakage loss with the increasing propagation distance.[22,23] Compared to the HE_{11} and TE_{01} (TM_{01}) modes, the HE_{31} mode with $n_{\rm eff}$ below 0.967 within $\beta\Lambda$ changing from 43 to 44 can distribute at the boundary between the air core and cladding region and it will constantly leak into the cladding region and attenuate through coupling with surface mode and resonating with the cladding structures. The corresponding two-dimensional transverse electric field distributions of guided-modes at appointed $\beta\Lambda$ of 43.6 are shown in Figs. 4(a), 4(b), and 4(c), respectively.

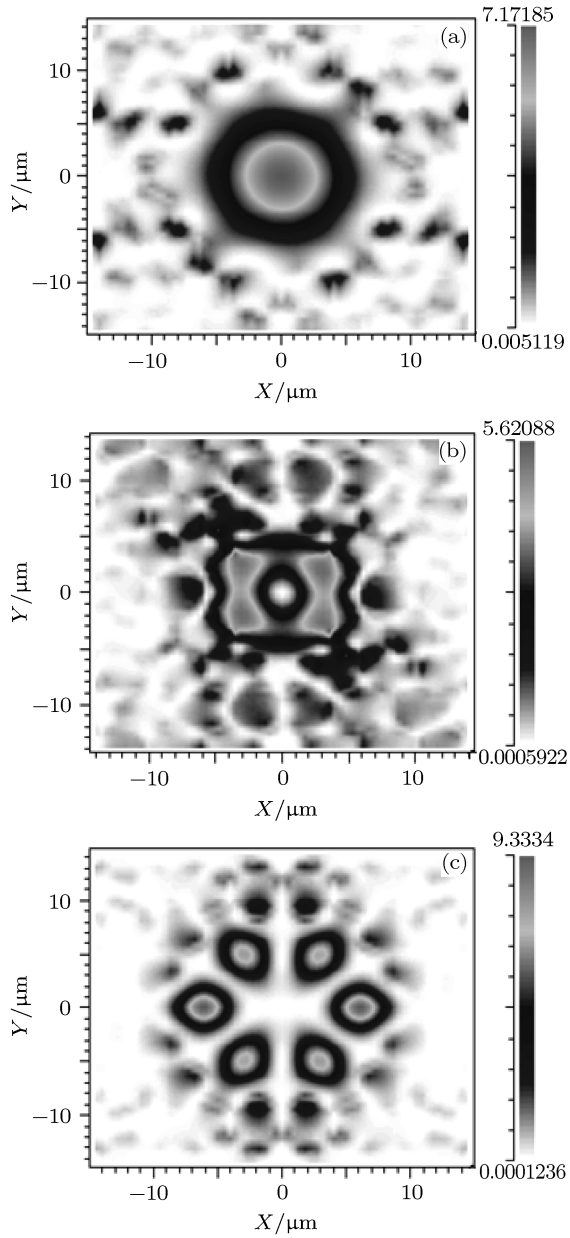


Fig. 4. The transverse electric field distributions of different order air guided-modes at appointed $\beta\Lambda$ of 43.6, (a), (b) and (c) displaying the distributions of HE_{11}, TE_{01} (TM_{01}) and HE_{31} modes, respectively.

As shown in Fig. 4(a), the transverse electric field distribution of the HE_{11} mode with n_{eff} 0.987 shows a Gauss-like shape consisting of a degenerate pair of quasi-uniformly polarized states (the doublet of HE_{11} mode) and the intensity reaches up to maximum at the centre of the fibre core, monotonically decrease with the distance from the centre. In Figs. 4(b) and 4(c), the electric field distribution of TE_{01} (TM_{01}) mode with n_{eff} 0.971 consisting of a degenerate pair of two-lobed modes (four-fold degenerate state including the doublet of HE_{21} mode and TE_0 and TM_0 mode with similar form but different frequencies) splits into two parts, while the HE_{31} mode with n_{eff} 0.964 splits into four parts and has more complex degenerate case. Because of interstitial holes's existence, the weak guidance theory can be well satisfied and the propagation characteristics of guided-modes are also similar to that of Bloch-modes. Especially the higher-order guided-modes (TE_{01}, TM_{01} and HE_{31} mode), which will constantly couple with the surface modes and leak out into the cladding region as the propagation distance increases and distribute over the whole cross section including holes and glass structure, exist in the forms of Bloch-mode.

Compared to the HE_{11} mode, the intensities of higher-order guided-modes in core region become weaker, diffuse toward the boundary between the air core and cladding region and tend to be noisier with more energy in the cladding structures. The setup of propagation experiment is shown in Fig. 5(a).

In the experiment, the tungsten–halogen lamp with the continuous spectrum range of 400 nm to 1700 nm and lower output intensity is used as a steady light source, as shown in Fig. 5(b). The lens system and coupling device are used to increase the coupling efficiency and a linear coupled charge device (CCD) is responsible for monitoring the output state. The pinhole diaphragm only permits the energy in air core to enter into the OSA. The length of HC-PBGF is 0.55 m and the propagation loss is measured about 0.045 dB/m at 600 nm by the cut-back method. With the OSA having a resolution of 0.1 nm, the transmission spectrum with wavelength range of 400 nm to 1200 nm is shown in Fig. 5(c). As shown in Fig. 5(c), the 3-dB transmitted intensities of 1st and 2nd PBGs labeled correspond to the wavelength ranges of 565 nm to 593 nm and 489 nm to 528 nm, which lay in the part band gaps of Fig. 2(b) (the corresponding wavelength ranges of 1st and 2nd PBGs in Fig. 2(b) are from 511 nm to 656 nm and 484 nm to 536 nm). Moreover, comparing Fig. 2(b) with Fig. 5(c), we find that some different band gaps exist, the main reasons are considered to be due to the discrepancies between simulation model and actual structure including the shape and size of holes and interstitial holes and the uniformity of transverse structure along lognitudinal direction.

Through choosing appropriate fibre length and adjusting the coupling device, two output near fields with a mixture of yellow and green light in the wavelength range of 565 nm to 593 nm, corresponding to the 1st PBG labeled in Fig .5(b), are observed using a line-array CCD by shielding the cladding region using a small hole-diaphragm, as shown in Fig. 6.

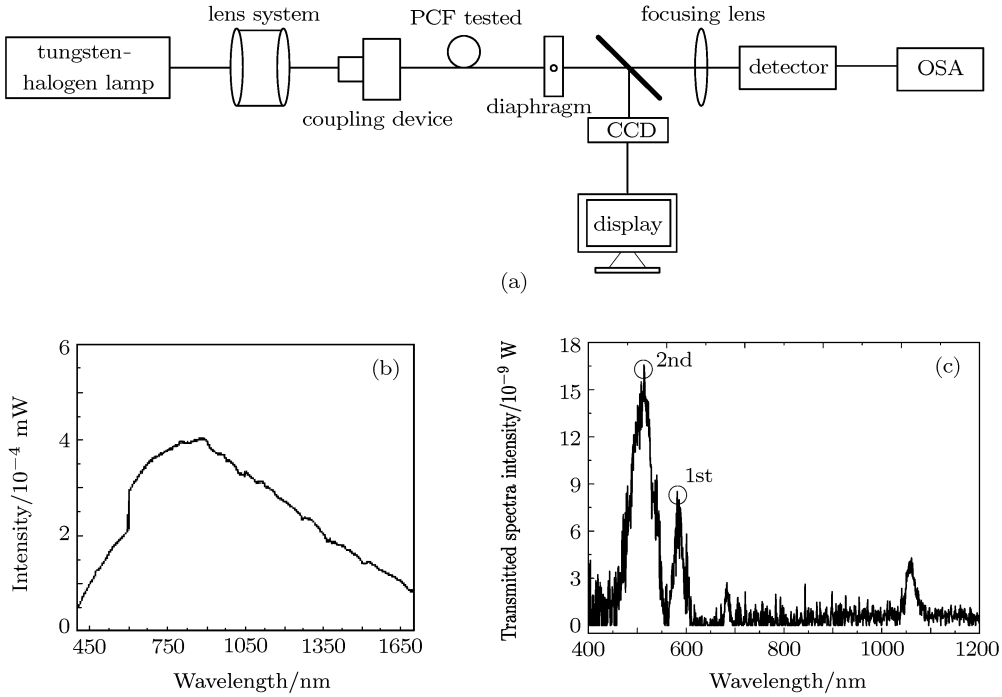


Fig. 5. (a) The experimental setup, panels (b) and (c) correspond to the spectrum of tungsten-halogen lamp and the transmission spectrum observed by optical spectrum analyser (OSA).

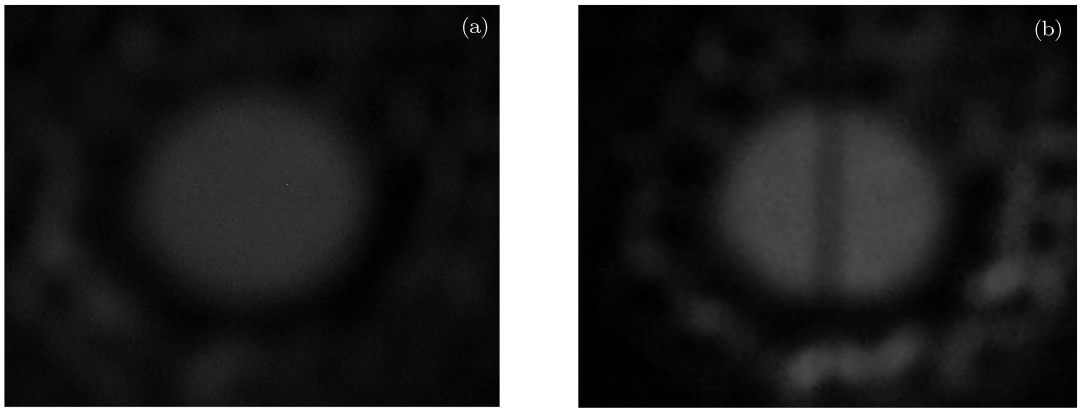


Fig. 6. The two output near-fields observed in experiment, (a) and (b) corresponding to the wavelength range from 565 nm to 593 nm.

The energy of output mode mainly comes from air core due to the cladding region being shielded, as shown in Figs. 6(a) and 6(b). In order to observe different order guided-modes, the fibre lengths are chosen as 0.55 m and 0.3 m with the coupling efficiency being adjusted to be above 50%. The output near fields of fundamental and second-order guided-modes correspond to the mode field distributions as shown in Figs. 4(a) and 4(b). The higher-order guided-modes are not observed due to higher propagation loss, but plenty of guided-modes can be excited and propagated due to larger core diameter and the existing case and loss mechanism are also complicated.

3. Discussion on loss of guided-modes

As discussed in Ref. [13], the loss limitations in HC-PBGF are mainly as a result of holey interface roughness scattering because of thermally excited surface capillary waves and the anti-crossing between the air guided-modes and surface modes.[24] The loss decrease in HC-PBGF guidance means the decrease of field strength of propagating modes at the holey interfaces due to holey interface roughness appearing to be an intrinsic property in the process of fibre drawing. One approach for it is to increase the air core size, which is limited by macro- or micro-bend loss[25,26]

constraints imposed by the undesirable guided-modes within the band gaps. With the increasing core size, the undesirable guide-modes gradually increase. The modal properties can be altered by proper design of the fibre geometry with a given core size and the most important one is the glass arrangement separating the core and cladding regions. In the process of fabrication, the thickness of core surround can be appropriately increased to achieve anti-resonance and the losses dominated by holey interface scattering can be further reduced. However, when the holey interface is smooth and the losses are dominated by mode coupling between guided-modes and boundary mode, the fibres with thicker core surrounds show an increased number of mode anti-crossing events due to larger amount of surface modes generated by truncation of infinite photonic crystal, which increases the coupling probability between the guided-modes and surface modes due to nearly equivalent propagation constants. The guided-modes will leak into the cladding region and attenuate gradually through resonating with the cladding structure including the glass interstitial apexes, the silica structures joining the neighbouring apexes and the air holes. In this case, it is very important to reduce the influence of surface modes. In our design and fabrication, the arrangement of capillaries is designed to make truncation of infinite photonic crystal reasonable and the electromagnetic boundary condition between core and cladding regions will not come into breaking. Moreover, the cladding structures are composed of thin-wall capillaries made of highly pure glass tube, the core is formed by extracting seven capillaries and the thinner core surround is beneficial to avoid surface modes. As shown in Figs. 6(a) and 6(b), no surface modes are observed. However, as a matter of fact, even if the surface modes can be eliminated, the guided-modes will also happen to leak due to finite cladding region and non-strict periodicity of cladding structures.

4. Conclusion

In summary, the guided-mode characteristics of HC-PBGF with interstitial holes fabricated in our lab at visible wavelengths are theoretically and experimentally investigated. The fundamental and second-order guided-modes are observed in experiment through choosing an appropriate fibre length and adjusting coupling device. The discrepancies between the simulation and experimental results are analysed and the loss mechanism of guided-modes in HC-PBGF is also discussed. The further works mainly concentrate on lowering the loss of such HC-PBGF to carry out application research on high power gas-filled laser and amplifier.

References

[1] Russell P St J 2003 *Science* **299** 358
[2] Knight J C 2003 *Nature* **424** 847
[3] Benabid F, Bouwmans G, Knight J C, Russell P St J and Couny F 2004 *Phys. Rev. Lett.* **93** 123903
[4] Benabid F, Light P S, Couny F and Russell P St J 2005 *Opt. Express* **13** 5694
[5] Hauri C P, Kornelis W, Helbing F W, Heinrich A, Couairon A, Mysyrowicz A, Biegert J and Keller U 2004 *Appl. Phys.* B **79** 673
[6] Hong K H, Hou B, Nees J, Power E and Mourou G 2005 *Appl. Phys.* B **81** 447
[7] Couny F, Benabid F and Light P S 2006 *Opt. Lett.* **31** 3574
[8] Kano P, Barker D and Brio M 2008 *J. Phys.* D: *Appl. Phys.* **41** 185106
[9] Cregan R F, Mangan B J, Knight J C, Birks T A, Russell P St J, Roberts P J and Allan D C 1999 *Science* **285** 1537
[10] Bouwmans G, Luan F, Knight J.C, Russell P St J, Farr L, Mangan B J and Sabert H 2003 *Opt. Express* **11** 1613
[11] Konorov S O, Zheltikov A M, Zhou P, Tarasevitch A P and vonder Linde D 2004 *Opt. Lett.* **29** 1521
[12] Couny F, Benabid F, Roberts P J, Burnett M T and Maier S A 2007 *Opt. Express* **15** 325
[13] Yuan J H, Yu C X, Sang X Z, Zhou G Y, Li S G and Hou L T 2009 *Appl. Phys.* B **96** 337
[14] Yuan J H, Hou L T, Zhou G Y, Wei D B, Chen C, Wang Q Y, Hu M L and Liu B W 2008 *Chin. Phys. Lett.* **25** 541
[15] Yuan J H, Hou L T, Zhou G Y, Wei D B, Chen C, Wang H Y, Dong S R, Wang Q Y, Liu B W and Hu M L 2008 *Acta Phys. Sin.* **57** 4230 (in Chinese)
[16] Mi Y, Hou L T, Zhou G Y, Wang K, Chen C, Gao F, Liu B W and Hu M L 2008 *Acta Phys. Sin.* **57** 3583 (in Chinese)
[17] Meng J, Hou L T, Zhou G Y, Gao F, Yuan J H and Wei D B 2008 *Chin. Phys.* B **17** 3779
[18] Zhou G Y, Hou Z Y and Hou L T 2006 *Appl. Opt.* **45** 4433
[19] Miyagi M, Hongo A, Aizawa Y and Kawakami S 1983 *Appl. Phys. Lett.* **43** 430
[20] Guo S P and Sacharia A 2003 *Opt. Express* **11** 167
[21] Ferrando A, Silvestre E, Miret J J andres P and Andres M V 1999 *Opt. Lett.* **24** 276
[22] Canning J, Buckley E, Lyytikainen K and Ryan T 2003 *Opt. Commun.* **205** 95
[23] Smith C M, Venkataraman N, Gallagher T M, Müller D, West J A, Borrelli N F, Allan D C and Koch K W 2003 *Nature* **424** 657
[24] Correa R A, Broderick N G R, Petrovich M N, Poletti F and Richardson D J 2006 *Opt. Express* **14** 7974
[25] Baggett J C, Monro T M, Furusawa K, Finazzi V and Richardson D J 2003 *Opt. Commun.* **227** 317
[26] Olszewski J, Szpulak M, Martynkien T, Urbanczyk W, Berghmans F, Nasiowski T and Thienpont H 2007 *Opt. Commun.* **269** 261